

The Photon and Light 1^{--} Mesons.

R.S. Longacre^a

^aBrookhaven National Laboratory, Upton, NY 11973, USA

Abstract

In this paper we look into the world data related to the photon and the connection to light mesons with the same spin parity quantum number as the photon $J^P = 1^-$.

1 Introduction to $\pi\pi$ scattering cross section

In this paper we use STAR high precision Au + Au ultra-peripheral coherent photoproduction collisions at $\sqrt{s_{NN}} = 200$ GeV (the highest RHIC energy)[1]. These photoproduction collisions produce pairs of pions ($\pi^+ \pi^-$ pairs) which are mainly in a $J^{pc} = 1^{--}$ quantum number system. We perform a global fit to the photoproduction combined with $e^+ e^-$ scattering to $\pi^+ \pi^-$ [2] and $\pi^+ \pi^- \pi^0$ [3]. To this fit we also use p-wave partial wave analysis of $\pi^+ \pi^-$ to $\pi^+ \pi^-$ [4].

The paper is organized in the following manner:

Sec. 1 is a introduction to $\pi\pi$ scattering cross section. Sec. 2 addresses re-scattering through the P-wave $\pi\pi$ which is a multi-channel problem. Sec. 3 is a global Söding model fit to all the Data. Sec. 4 we find 5 S-matrix poles in the $J^{pc} = 1^{--}$ quantum system. Sec. 5 we go beyond the Söding model and break up the photoproduction amplitude into its component parts and show how they are different in the lower mass and higher mass regions. Sec. 6 presents the summary and discussion.

1.1 $\pi\pi$ scattering cross section

For the first part of this story we will define what a scattering cross section is. We will first only consider elastic scattering of pions. Two pions can scatter at a certain energy which we will call $M_{\pi\pi}$. The differential cross section σ at a given $M_{\pi\pi}$ is

$$\frac{d\sigma}{d\phi d\theta} = \frac{1}{K^2} \left| \sum_{\ell} (2\ell + 1) T_{\ell} P_{\ell}(\cos\theta) \right|^2 \quad (1)$$

where ϕ and θ are the azimuthal and scattering angles, respectively. T_{ℓ} is a complex scattering amplitude and ℓ is the angular momentum. P_{ℓ} is the Legendre polynomial, which is a function of $\cos\theta$. K is the flux factor equal to the pion momentum in the center of mass. The T_{ℓ} elastic scattering amplitudes are complex amplitudes described by two real numbers one bounded between 0.0 and 1.0 (η_{ℓ}) and another is in units of angles (δ_{ℓ}). The form of the amplitude is

$$T_{\ell} = \eta_{\ell} \sin\delta_{\ell} e^{i\delta_{\ell}} \quad (2)$$

We note that η_{ℓ} and δ_{ℓ} depends on the value of ℓ and $M_{\pi\pi}$.

2 Re-scattering through the P-wave $\pi \pi$ is a multi-channel problem

In order to handle the multi-channel problem which exist in P-wave $J^{pc} = 1^{--}$ we will use the K-matrix approach. When we are below the $\pi \pi \pi$ threshold the system is only a one channel problem and the K-matrix is only a single term of the matrix however as we move up in energy more channels open up. Also the 1^{--} couples to the photon which can couple to pairs of electrons(e^+e^-). and muons($\mu^+\mu^-$). Below is a table of channels we will use in our K-matrix approach.

Table I. The channels used and the number assigned to them.

Table I	
channel particles	channel number
$\pi^+\pi^-$	1
$\pi^+\pi^-\pi^0$	2
e^+e^-	3
$\mu^+\mu^-$	4
$\eta \pi^+\pi^-$	5

Ordinarily in a hadronic K-matrix there would be a unique set of quantum numbers which includes isospin. However with the coupling of the photon we have isospin mixing. The isospin of the $\pi^+ \pi^-$ system is $I = 1$. The $\pi^+ \pi^- \pi^0$ system is $I = 0$. The $\eta \pi^+ \pi^-$ system is $I = 1$. The e^+e^- and $\mu^+\mu^-$ couples to both isospins and have a universal coupling through the photon.

The 1^{--} P-wave $\pi \pi$ couples mainly to the $\rho(760)$ and can with first blush be considered a single channel problem. Such a k-matrix would be given by,

$$K_{11} = \tan\delta_0. \quad (3)$$

We see that when $\delta_0 = 90^\circ$ that there will be a pole in the K-matrix and in this case the $\rho(760)$.

$$K_{11} = \frac{\frac{2\gamma_1^2 Z_1^2 q_1}{(Z_1^2+1)M_{\pi\pi}}}{(M_1^2 - M_{\pi\pi}^2)}. \quad (4)$$

Where γ_1 is the coupling of the pole($\rho(760)$) to the $\pi\pi$ channel, $q_1 = q_{\pi\pi}$ is the center of mass momentum of the $\pi\pi$ channel with Z_1 as the ratio of the center mass momentum q_1 divided by q_s which is .200 GeV/c(size of 1.0 fm), also M_1 is the mass of the pole($\rho(760)$), The T-matrix is given by

$$T_{11} = e^{i\delta_0} \sin\delta_0 = \frac{K_{11}}{(1 - iK_{11})} = (1 - iK)^{-1}K. \quad (5)$$

2.1 Low Mass Region(threshold to 1.1Gev)

The $\rho(760)$ couples to four of the five channels which we consider in this paper. Each of channels have a phase space factor. For channel 1($\pi\pi$) we had $\frac{2Z_1^2 q_1}{(Z_1^2+1)M_{\pi\pi}}$ on the previous page. For channel 2($\pi\pi\pi$) we have $\frac{2Z_2^2 q_2}{(Z_2^2+1)M_{\pi\pi}}$, where q_2 is the center mass momentum of two pions at rest to the other pion. Here we use $m_{\pi\pi}$ to register energy of the system which is the same in all channels. Z_2 is the ratio of q_2 to q_s . Channel 3(e^+e^-) we have $\frac{2q_3}{M_{\pi\pi}}$, where q_3 is the center mass momentum of the e^+e^- system. Channel 4($\mu^+\mu^-$) we have $\frac{2q_4}{M_{\pi\pi}}$, where q_4 is the center mass momentum of the $\mu^+\mu^-$ system.

Isospin mixing is part of this four channel $j^{pc} = 1^{--}$. the isospin partner of the $\rho(760)$ is the $\omega(783)$. We need two k-matrix poles where pole 1 is the $\rho(760)$ and pole 2 is the $\omega(783)$. The k-matrix is given by

$$K_{11} = \sum_i \frac{\frac{2\gamma_{i1}^2 Z_1^2 q_1}{(Z_1^2+1)M_1}}{(M_i^2 - M_1^2)}, K_{22} = \sum_i \frac{\frac{2\gamma_{i2}^2 Z_2^2 q_2}{(Z_2^2+1)M_1}}{(M_i^2 - M_1^2)}, K_{33} = \sum_i \frac{\frac{2\gamma_{i3}^2 q_3}{M_1}}{(M_i^2 - M_1^2)}, K_{44} = \sum_i \frac{\frac{2\gamma_{i4}^2 q_4}{M_1}}{(M_i^2 - M_1^2)}. \quad (6)$$

An example of a cross term

$$K_{12} = \sum_i \frac{\frac{2\gamma_{i1}\gamma_{i2}\sqrt{Z_1^2 Z_2^2 q_1 q_2}}{\sqrt{(Z_1^2+1)(Z_2^2+1)M_1^2}}}{(M_i^2 - M_1^2)}. \quad (7)$$

The T-matrix is given by

$$T = (\delta - iK)^{-1}K. \quad (8)$$

The universal lepton coupling through the photon means that $\gamma_{i3} = \gamma_{i4}$.

2.2 High Mass Region(1.1Gev to 1.9Gev)

For the high mass region we use a factorizable k-matrix(k_1, k_2, k_3, k_4, k_5), such that

$$K_{ij} = k_i k_j. \quad (9)$$

We use a 9th order polynomial as a function of $M_{\pi\pi}$ for k_1 and starting with the values generated from Ref.[4] see the appendix. For k_2 we use zero coupling assuming that the only three pion state is the $\omega(783)$ which is very narrow and confined to the lower mass region. for k_3 and k_4 we use the same simple linear function of $M_{\pi\pi}$ since we have universal lepton coupling through the photon. For k_5 we use the 9th order polynomial starting values

generated from Ref.[4] see the appendix where we use for k_5 the k-matrix element denoted by k_2 .

3 A Global Söding Model Fit to all the Data

We perform a global fit to the coherent photoproduction data using a generalized Söding Model[5] plus $e^+ e^-$ scattering to $\pi^+ \pi^-$ [2] and $\pi^+ \pi^- \pi^0$ [3]. To this fit we also use p-wave partial wave analysis of $\pi^+ \pi^-$ to $\pi^+ \pi^-$ [4]. The 4 channel k-matrix is used for low mass region and the 5 channel for high mass region as set up in last section. We fit directly to the T_{11} Argand plot of Ref.[4]. As part of the global fit we also fit Ref.[2] and Ref.[3] using

$$CrossSection_{\pi\pi} = \frac{C}{p_{ee}} |T_{31}|^2, \quad (10)$$

and

$$CrossSection_{\pi\pi\pi} = \frac{C}{p_{ee}} |T_{32}|^2. \quad (11)$$

The photoproduction data are fitted using a generalized Söding Model[5] which is outlined in Figure 1. We see in the figure that there are two terms. One being a Söding background term of pion pairs coming directly out of the vacuum plus a second being the photon coupling directly to the 1^{--} scattering matrix. The universal lepton pair coupling through the photon gives us T_{31} as the direct coupling. We use the form for the Söding background term given by

$$B_{\pi\pi} = b_{\pi\pi} \sqrt{\frac{2p_{\pi\pi}}{M_{\pi\pi}}} e^{-d_{\pi\pi} M_{\pi\pi}}. \quad (12)$$

The directly coupled term of the photon to the S-matrix is given by

$$CT_{31} = c \sqrt{\frac{M_{\pi\pi}}{2p_{ee}}} T_{31}. \quad (13)$$

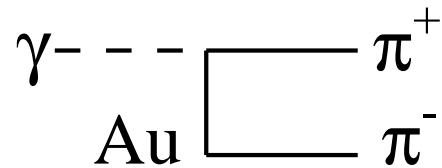
The results of the global fit is shown in Figures 2 through 6. The overall χ^2 for the global fit which has 1669 degrees of freedom is 1926. The 1σ error on such a fit is a $\Delta\chi^2$ of 58. This implies that this global fit is 4.8σ away from a 1669 χ^2 fit.

$$\gamma \text{ Au} \rightarrow \pi^+ \pi^- \text{ Au}$$

Söding model

Sum of two amplitudes

background term $B_{\pi\pi}$



Direct production $C T_{31}$

$$A = B + C T_{31}$$

Figure 1: The Söding Model[5] is made up of two terms. the first term is a direct formation of $\pi^+ \pi^-$ from the photon, which is depicted in the diagram above. The second term is the photon going into quarks and then into $\pi^+ \pi^-$. For this term we use $e^+ e^-$ scattering to $\pi^+ \pi^-$ [2] as stand in for this formation(T_{31}).

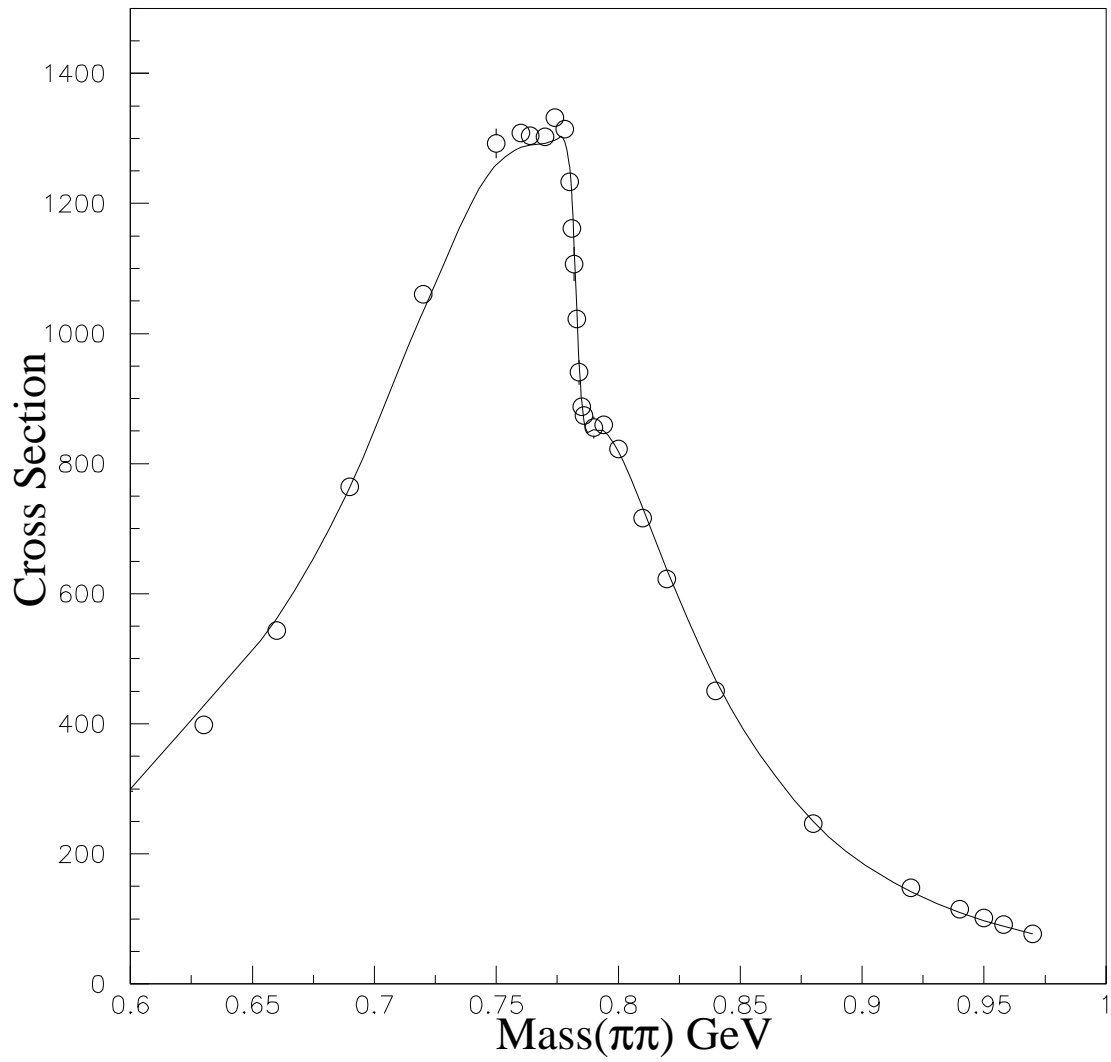


Figure 2: The scattering cross section of $e^+ e^-$ scattering to $\pi^+ \pi^-$ [2] and our global fit described in the text.

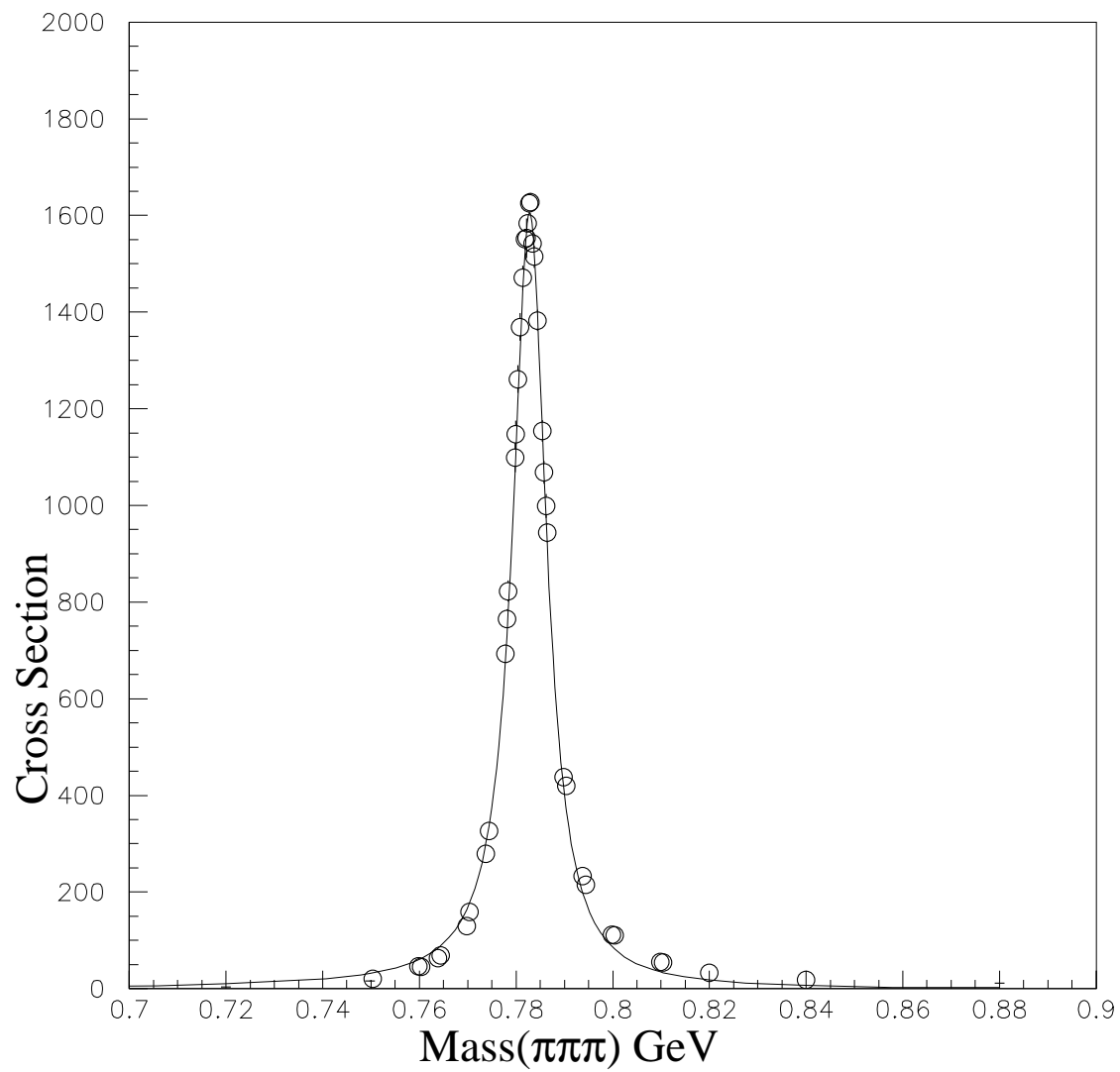


Figure 3: The scattering cross section of $e^+ e^-$ scattering to $\pi^+ \pi^- \pi^0[3]$ and our global fit described in the text.

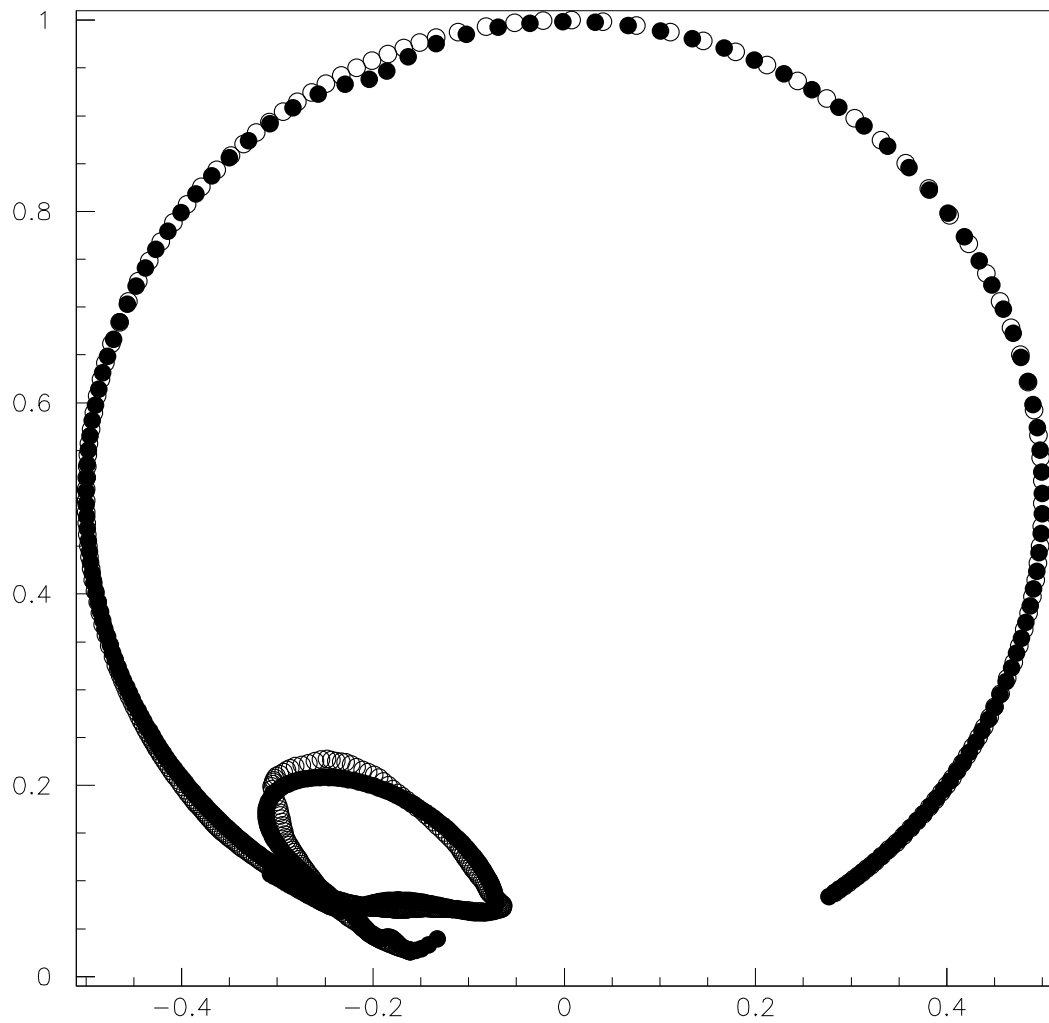


Figure 4: The Argand plot of the S-matrix p-wave partial wave analysis of $\pi^+ \pi^-$ to $\pi^+ \pi^-$ [4]. The input amplitude are open dots(\circ) and our global fit described in the text are solid dots (\bullet).

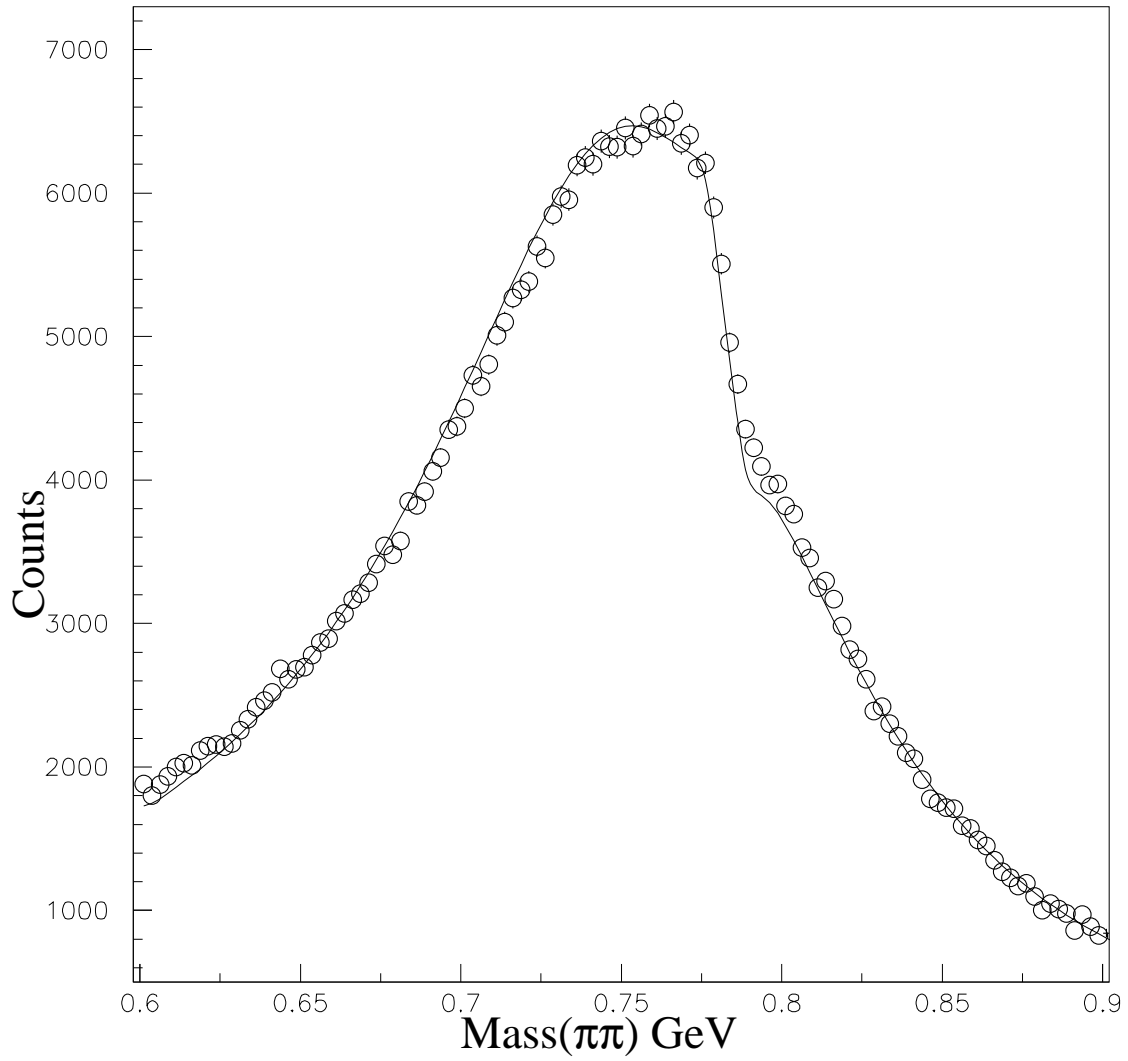


Figure 5: The STAR high precision Au + Au ultra-peripheral coherent photoproduction data at $\sqrt{s_{NN}} = 200$ GeV (the highest RHIC energy) for the lower mass region 0.6 GeV to 0.9 GeV and our global fit described in the text.

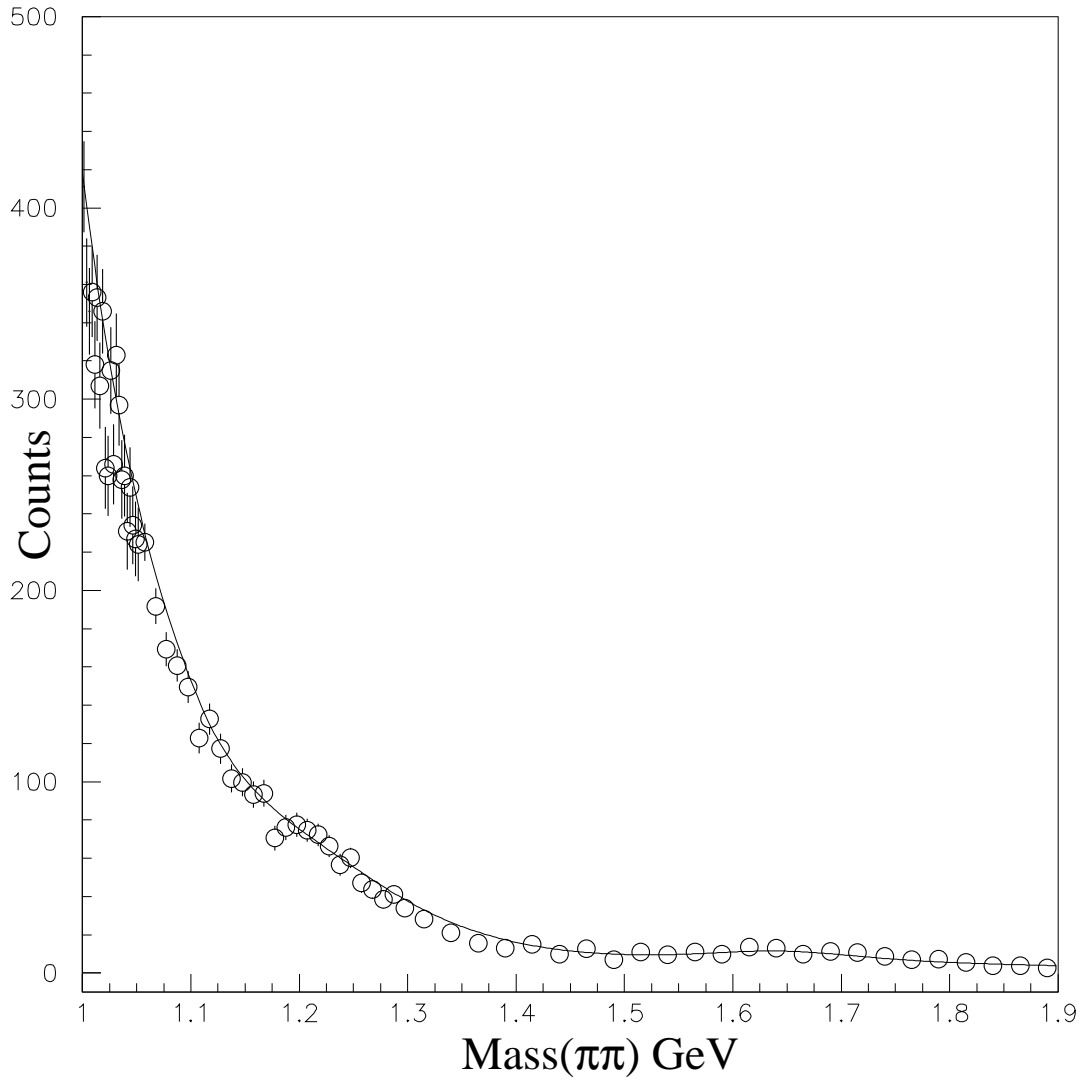


Figure 6: The STAR high precision Au + Au ultra-peripheral coherent photoproduction data at $\sqrt{s_{NN}} = 200$ GeV (the highest RHIC energy) for the higher mass region 1.0 GeV to 1.9 GeV and our global fit described in the text.

4 Poles of the 1^{--} S-Matrix

In the above section we have achieved a global fit to the data sets which includes the STAR high precision Au + Au ultra-peripheral coherent photoproduction collisions into pairs of pions ($\pi^+ \pi^-$ pairs) plus $e^+ e^-$ scattering to $\pi^+ \pi^-$ [2] and $\pi^+ \pi^- \pi^0$ [3]. To this fit we also fit p-wave partial wave analysis of $\pi^+ \pi^-$ to $\pi^+ \pi^-$ [4]. With this fit we have achieved an analytic form for the S-matrix. Using this analytic form we search for poles in the 1^{--} S-matrix. In this search we find 5 poles.

Table II. Poles of the 1^{--} S-Matrix.

Table II					
mass	width	$\pi \pi$	$\pi \pi \pi$	$e^+ e^-$	other
$0.764 GeV$	$.148 GeV$	100	0	.0047	0
$0.783 GeV$	$.008 GeV$	2	89	.0074	9
$1.333 GeV$	$.334 GeV$	5.4	0	.0000015	94.6
$1.629 GeV$	$.221 GeV$	19	0	.0000039	81
$1.733 GeV$	$.246 GeV$	7.5	0	.00000083	92.5

The first pole is the well known $\rho(760)$, while its isospin partner $\omega(780)$ is the second pole. In the table for the $\omega(780)$ the decay mode for this state marked as other is the radiative decay mode $\gamma \pi$. The branching fractions are measured in percentage.

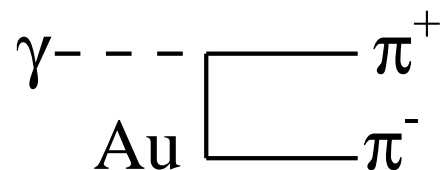
In the high mass region one expects there should be two radial excitations of the $\rho(760)$. These excitation masses should be at around 1300 and 1800 MeV. One should also expect there should be a d-wave $q \bar{q}$ state at around 1600 MeV. We see the poles in the high mass are consistent with this picture. .

5 Beyond the Söding Model Fit.

The Söding Model has a built-in term of interference between the direct production term and the background term. This interference term is equivalent to a re-scattering as shown in Figure 7. The re-scattering term is a loop of pions coming from the background and re-interacting with the S-matrix of $\pi \pi$ p-wave scattering. The loop or bubble has a real and an imaginary part. The imaginary part of the loop is equal to $B_{\pi\pi}$ (equation 12) times S-matrix $\pi \pi$ p-wave scattering. The real part of the loop is equal to $\alpha B_{\pi\pi}$ times S-matrix $\pi \pi$ scattering. The value of α is determined to be 2.0 in Ref.[6] from photo production data. Figure 7 and equation 14 gives the equation for the background plus re-scattering

$$T = 2.0B_{\pi\pi}T_{11} + B_{\pi\pi}(1.0 + iT_{11}). \quad (14)$$

$$\gamma \text{ Au} \rightarrow \pi^+ \pi^- \text{ Au}$$



background term $B_{\pi\pi}$



rescattering bubble

$$T = \alpha B_{\pi\pi} T_{11} + B_{\pi\pi} (1 + iT_{11})$$

Figure 7: Beyond the Söding Model we focus on two terms one being a direct formation of $\pi^+ \pi^-$ from the photon and the other being the re-scattering through the S-matrix of $\pi \pi$ p-wave scattering. The loop or bubble has a real and a imaginary part. This leads to the above equation.

5.1 The Lower Mass region

To the above term we must add the direct production of the $\rho(760)$ pole and the $\omega(780)$ pole in the lower mass region. When this is done we break the constraint of the Söding Model that the $\omega(780)$ into $\pi\pi$ has to be the same as e^+e^- scattering to $\pi^+\pi^-$ [2]. With this added freedom the global fit χ^2 improve by 257 which a 4.8σ improvement (see Figure 8). This photo production amplitude into $\pi\pi$ is shown in Figure 9, while the Söding Model $\pi\pi$ amplitude is shown in Figure 10. Even though we have a quantitative difference these amplitudes are qualitatively the same.

5.2 The Higher Mass region

In the higher mass region a new background becomes possible. In our model for the 1^{--} system we have a large coupling of the $\pi\pi$ channel to the $\eta\pi\pi$ channel. Thus if the photon directly produces the $\eta\pi\pi$ channel, then through a $\eta\pi\pi$ loop one can form the $\pi\pi$ channel by the cross term of the S-matrix of $\eta\pi\pi$ to $\pi\pi$ (see Figure 11). Again the loop or bubble has a real and a imaginary part. The imaginary part of the loop is equal to $B_{\eta\pi\pi}$ (equation 15) times T-matrix $\eta\pi\pi$ to $\pi\pi$ scattering. The real part of the loop is equal to $2.0 B_{\eta\pi\pi}$ times T-matrix $\eta\pi\pi$ to $\pi\pi$. Figure 11 and equation 16 gives the equation for the re-scattering

$$B_{\eta\pi\pi} = b_{\eta\pi\pi} \sqrt{\frac{2p_{\eta\pi\pi}}{M_{\pi\pi}}} e^{-d_{\eta\pi\pi} M_{\pi\pi}}. \quad (15)$$

$$T = 2.0 B_{\eta\pi\pi} T_{51} + i B_{\eta\pi\pi} T_{51}. \quad (16)$$

We perform a new global fit to the photoproduction data plus e^+e^- scattering to $\pi^+\pi^-$ [2] and $\pi^+\pi^-\pi^0$ [3] plus the p-wave partial wave analysis of $\pi^+\pi^-$ to $\pi^+\pi^-$. As part of this fit we use equation 14 and equation 16. Since the photoproduction data is the square of the amplitude there is an over all phase that is not determined. Let us choose equation 14 to determine this phase. The result of this fit gives a result for equation 14 which is displayed in Figure 12. The background rises quickly at threshold and then falls off with mass. The higher mass region is the focus of Figure 13. We see that the background term equation 14 for the pion loop is mainly a real function. Equation 16 which is the $\eta\pi\pi$ loop is also mainly real and of the same magnitude at these higher masses. This background also rises quickly at threshold and then falls off with mass tailing to zero (see Figure 14).

5.3 The Higher Mass Region Poles and Unitarity

In the S-matrix in the higher mass region there are 3 poles plus the possibility of background terms when we consider T_{11} and T_{51} . Unitarity means that all of these terms must fit together and satisfy the unitary constraints. We are able to achieve such an unitary construction using an ad hoc step by step construction of first T_{11} and then T_{51} . The tail of the $\rho(760)$

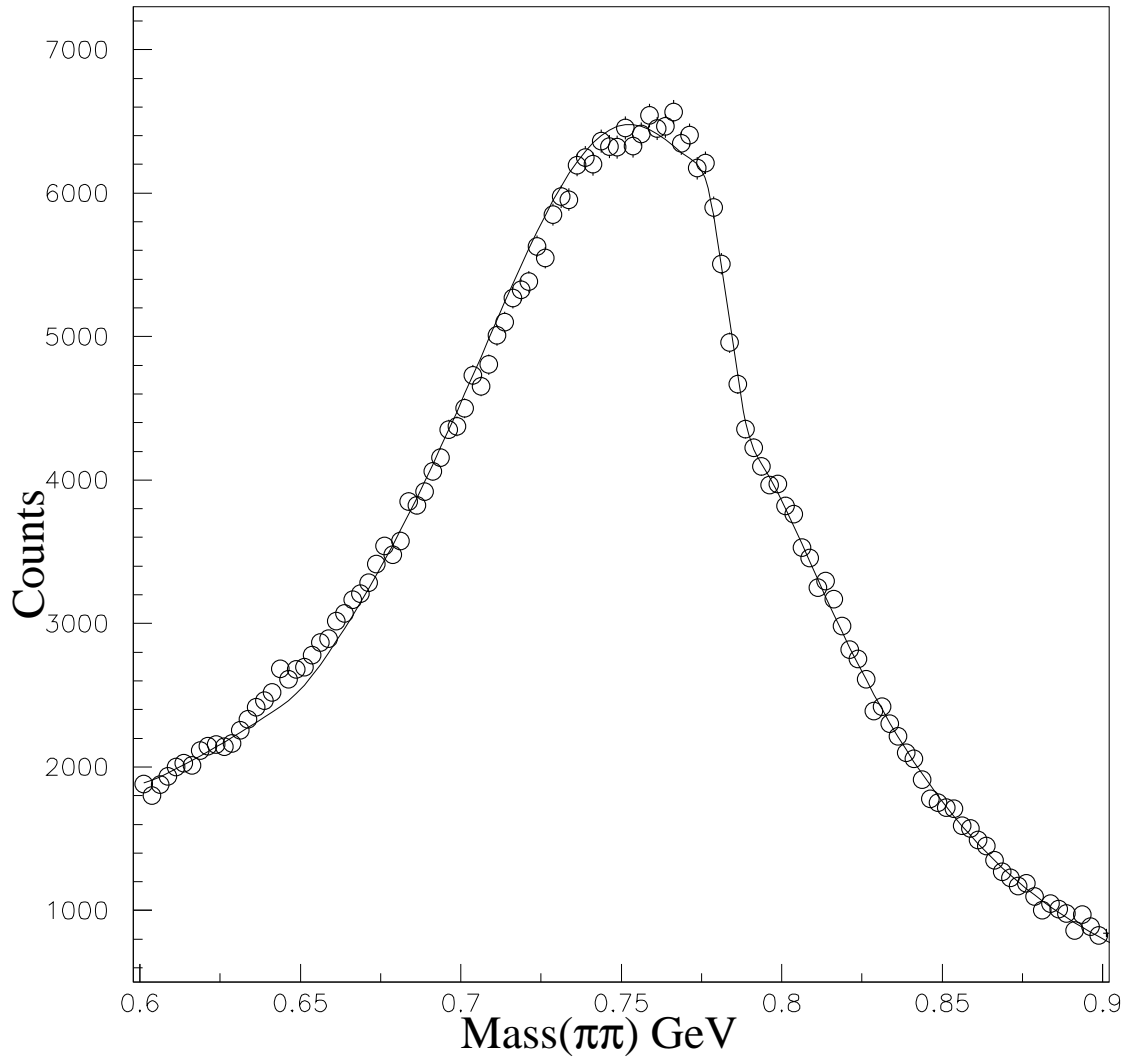


Figure 8: The STAR high precision Au + Au ultra-peripheral coherent photoproduction data at $\sqrt{s_{NN}} = 200$ GeV (the highest RHIC energy) for the lower mass region 0.6 GeV to 0.9 GeV and our global fit with re-scattering bubbles and direct production of poles as described in the text.

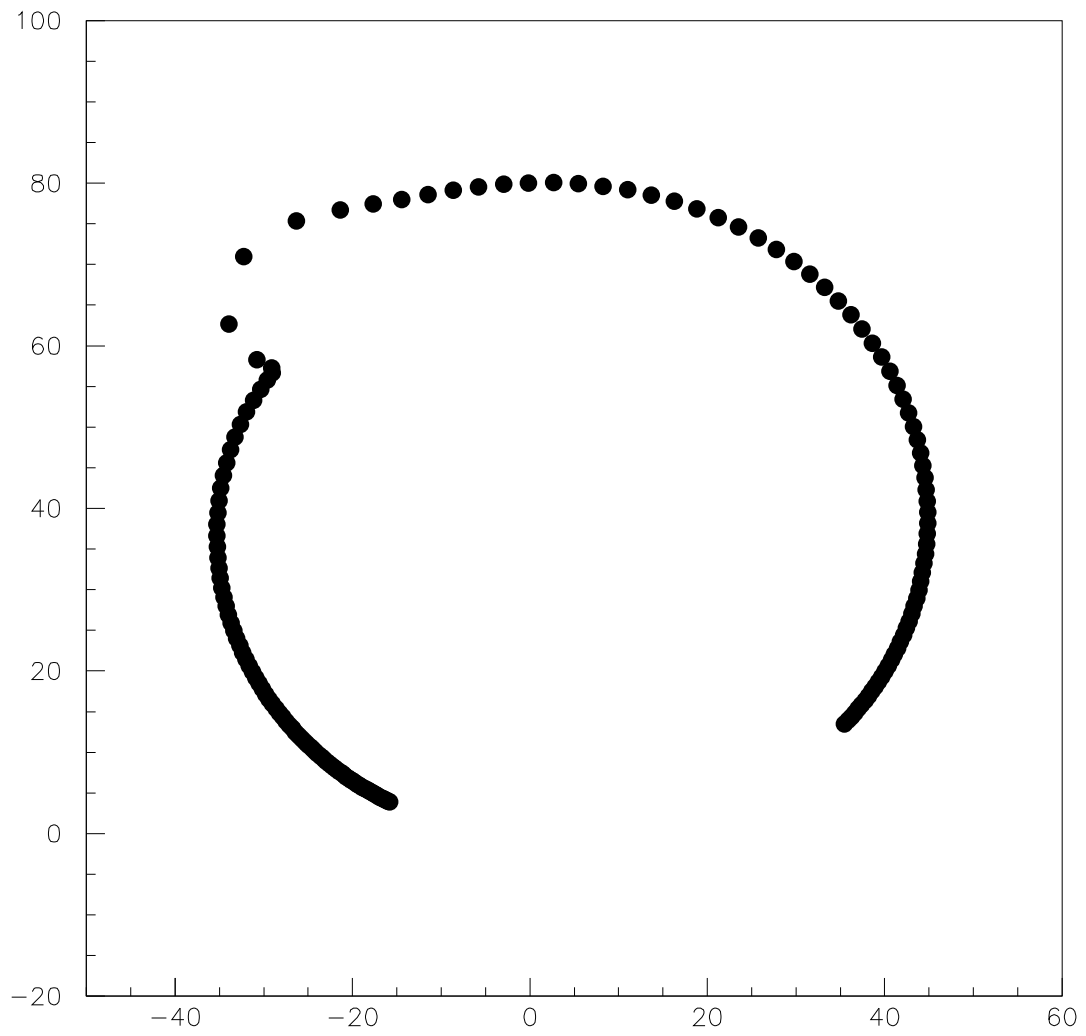


Figure 9: The Argand plot of the amplitude of the photoproduction fit with re-scattering bubbles and direct production of poles in the lower mass region 0.6 GeV to 0.9 GeV as described in the text is shown.

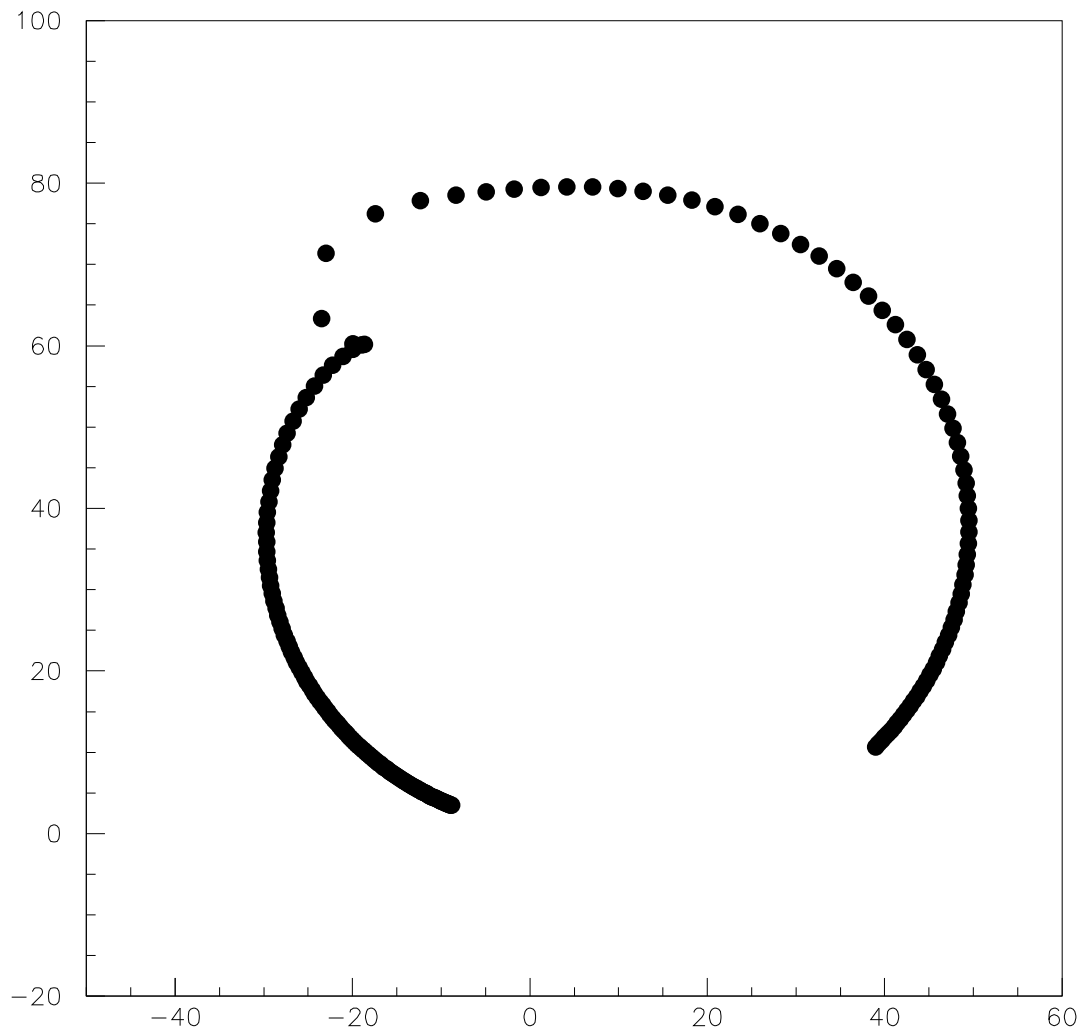
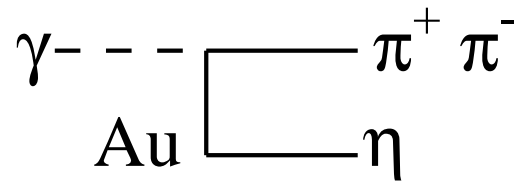


Figure 10: The Argand plot of the amplitude of the photoproduction fit from the Söding Model in the lower mass region 0.6 GeV to 0.9 GeV as described in the text is shown and should be compared with Figure 9.

$$\gamma \text{ Au} \rightarrow \eta \pi^+ \pi^- \text{ Au}$$



background term $B_{\eta\pi\pi}$



rescattering bubble

$$T = 2B_{\eta\pi\pi} T_{51} + iB_{\eta\pi\pi} T_{51}$$

Figure 11: Beyond re-scattering through $\pi \pi$ loops we focus on two terms one being a direct formation of $\eta \pi \pi$ from the photon and the other being the re-scattering through the S-matrix of $\eta \pi \pi$ to $\pi \pi$. The loop or bubble has a real and a imaginary part. This leads to the above equation.

meson extend into the high mass region tailing off to a small amplitude. We will denote this background as B_{11} . The shape of this background is shown in Figure 15. The poles for $\rho(1330)$ and $\rho(1730)$ have a very small coupling to the $\pi\pi$ channel. For these poles we use a Breit-Wigner form which has the same pole position as our k-matrix fit. Let us denote these forms as $BW_1(\rho(1330))$ and $BW_3(\rho(1730))$. We define the quasi factorizable Breit-Wigner form($B\tilde{W}_2$) through the equation

$$B\tilde{W}_2 = T_{11} - B_{11} - C_{111}BW_1 - C_{113}BW_3. \quad (17)$$

where C_{111} is a complex constant that makes the $\rho(1330)$ pole residue the same as the k-matrix fit, and C_{113} is also a complex constant that makes the $\rho(1730)$ pole residue the same. We turn to the T_{51} amplitude and define a background term B_{51} such that

$$B_{51} = T_{51} - C_{512}B\tilde{W}_2 - C_{511}BW_1 - C_{513}BW_3. \quad (18)$$

The above equation has the constraint

$$REAL(T_{51} - C_{512}B\tilde{W}_2 - C_{511}BW_1 - C_{513}BW_3) \approx 0. \quad (19)$$

The final fit to the high mass photoproduction data is given by

$$T = 2.0B_{\pi\pi}T_{11} + B_{\pi\pi}(1.0 + iT_{11}) + C_1T_{51} + C_2B_{11} + C_3B_{51} + C_4BW_1 + C_5BW_3 + C_6B\tilde{W}_2. \quad (20)$$

The $B_{\pi\pi}$ is a real constant and $C_1, C_2, C_3, C_4, C_5, C_6$ are complex constants. The results of the eight terms are shown in figures 13 through 19 with the final sum being Figure 20 with the fit shown in Figure 21. The overall χ^2 for this global fit which has 1649 degrees of freedom is 1649. In the higher mass region we get an improvement of 20 in χ^2 . This is a better fit than before but not statistical significant. We can compare with the higher mass amplitude from the Söding Model fit which we show in Figure 22.

6 Summary and Discussion

We have perform a global fit to the photoproduction data using a generalized Söding Model[5] plus e^+e^- scattering to $\pi^+\pi^-$ [2] and $\pi^+\pi^-\pi^0$ [3]. To this fit we also use p-wave partial wave analysis of $\pi^+\pi^-$ to $\pi^+\pi^-$ [4]. The 4 channel k-matrix is used for low mass region and the 5 channel for high mass region as set up in section 2. We fit directly to the T_{11} Argand plot of Ref.[4]. As part of the global fit we also fit Ref.[2] and Ref.[3] using equation 10 and 11.

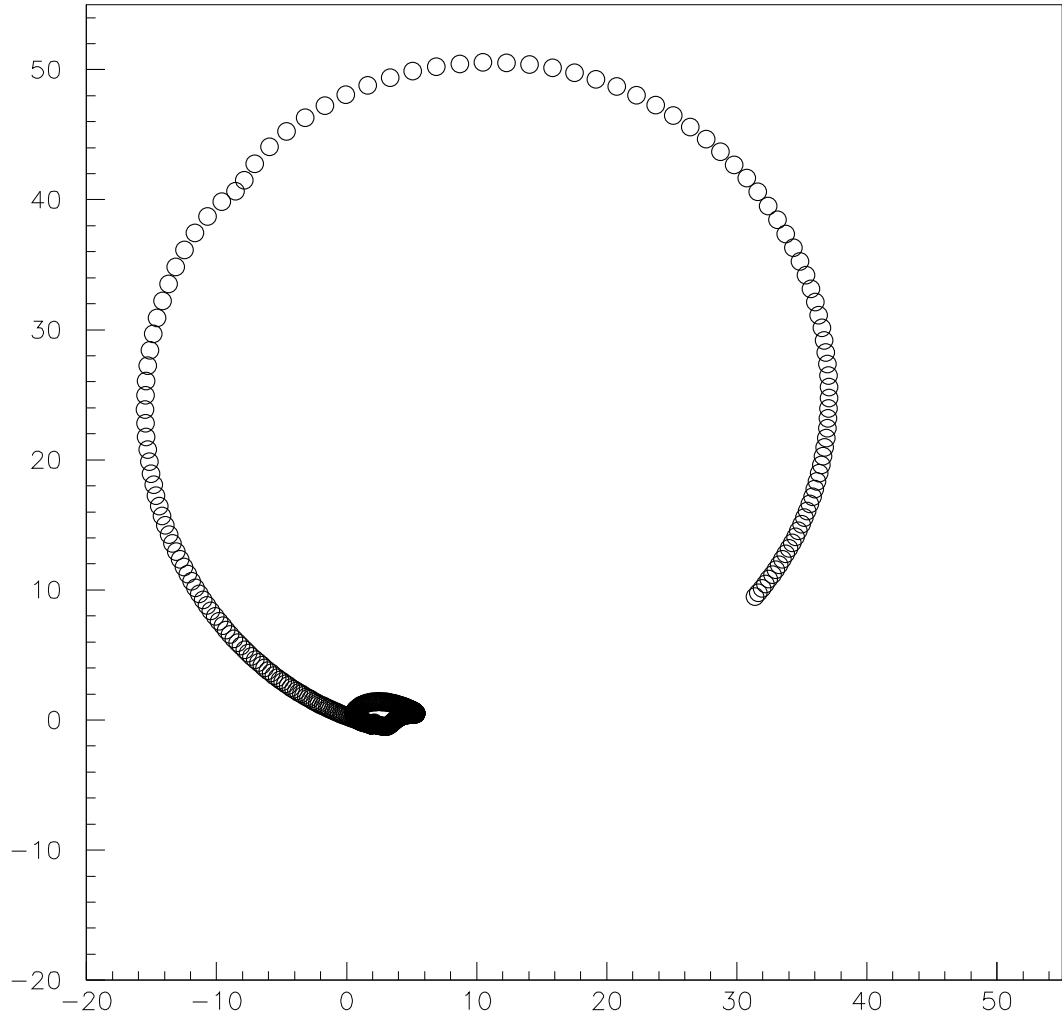


Figure 12: Equation 14 has two terms one being a direct formation of $\pi^+ \pi^-$ from the photon and the other being the re-scattering through the S-matrix of $\pi \pi$ p-wave scattering. This loop or bubble has a real and a imaginary part. In the fit of equation 20 to the STAR high precision Au + Au ultra-peripheral coherent photoproduction data at $\sqrt{s_{NN}} = 200$ GeV (the highest RHIC energy) we obtain the above amplitude for equation 14.

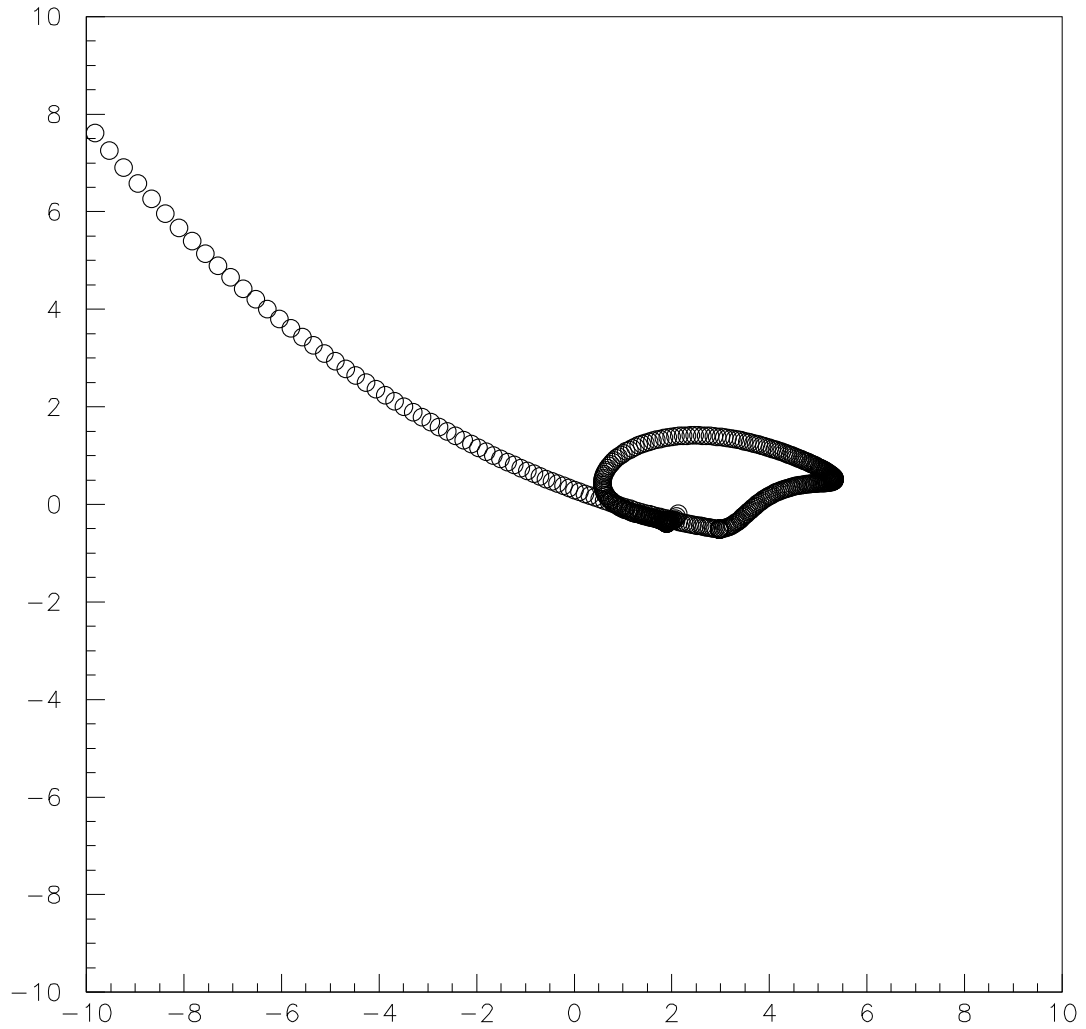


Figure 13: Equation 14 has two terms one being a direct formation of $\pi^+ \pi^-$ from the photon and the other being the re-scattering through the S-matrix of $\pi \pi$ p-wave scattering. This loop or bubble has a real and a imaginary part. In the fit of equation 20 to the STAR high precision Au + Au ultra-peripheral coherent photoproduction data at $\sqrt{s_{NN}} = 200$ GeV (the highest RHIC energy) we obtain the above equation 14 amplitude for the higher mass region 1.0 GeV to 1.9 GeV.

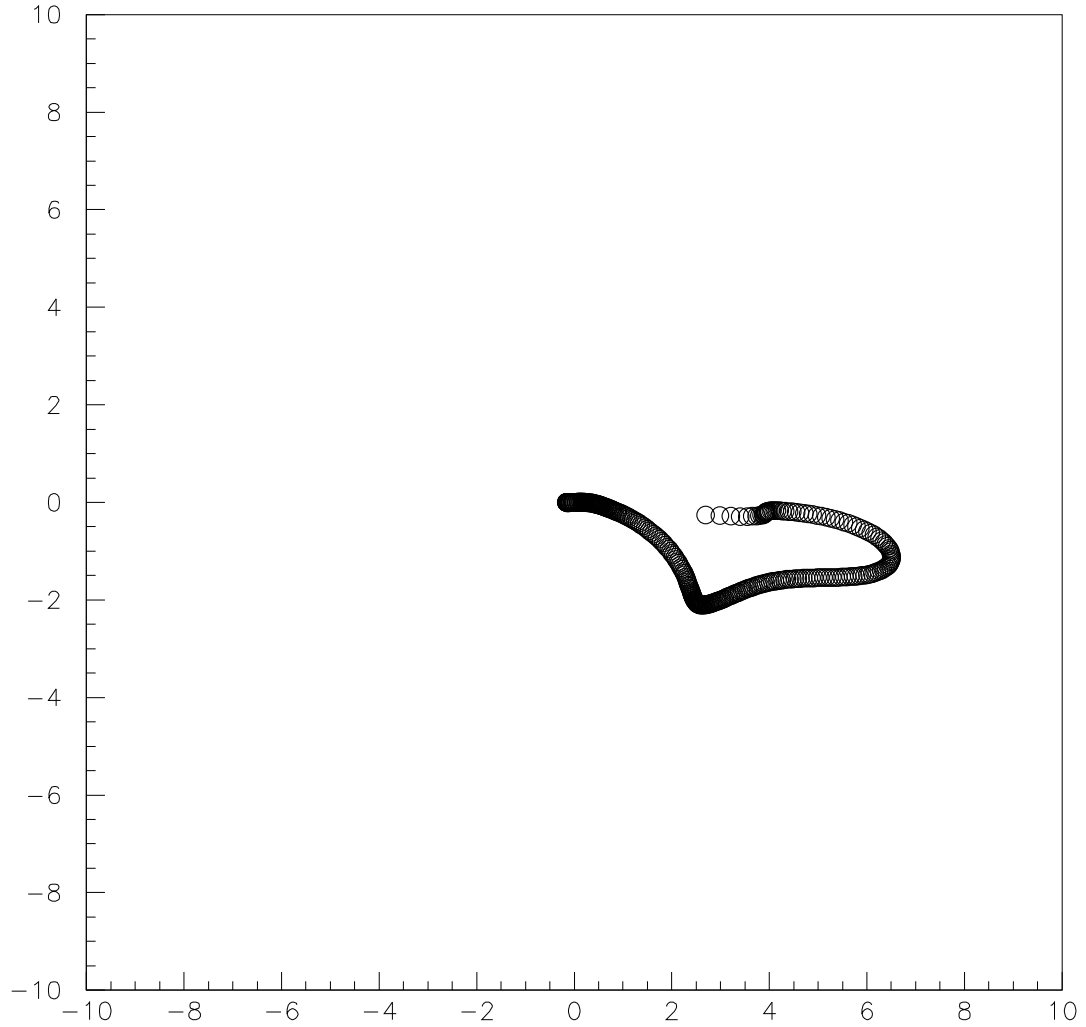


Figure 14: Equation 16 has two terms coming from a loop or bubble re-scattering through the S-matrix of $\eta \pi \pi$ to $\pi \pi$. The loop or bubble has a real and a imaginary part. In the fit of equation 20 to the STAR high precision Au + Au ultra-peripheral coherent photoproduction data at $\sqrt{s_{NN}} = 200$ GeV(the highest RHIC energy) we obtain for the third term(equation 16) the above amplitude for the higher mass region 1.0 GeV to 1.9 GeV.

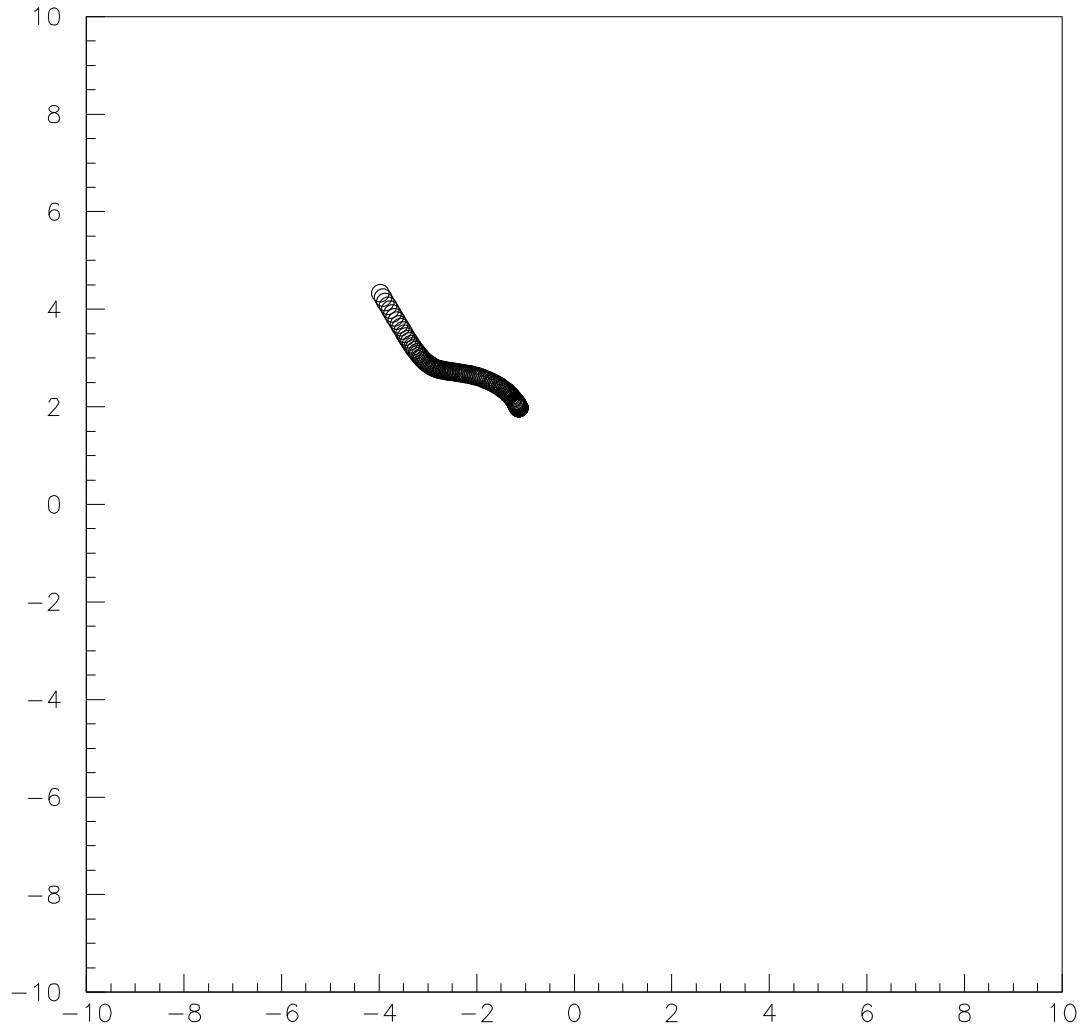


Figure 15: In the S-matrix $\pi \pi$ to $\pi \pi$ there is a smooth background term which is used in equation 20(the fourth term). In the fit of equation 20 to the STAR high precision Au + Au ultra-peripheral coherent photoproduction data at $\sqrt{s_{NN}} = 200$ GeV(the highest RHIC energy) we obtain for the fourth term the above amplitude for the higher mass region 1.0 GeV to 1.9 GeV.

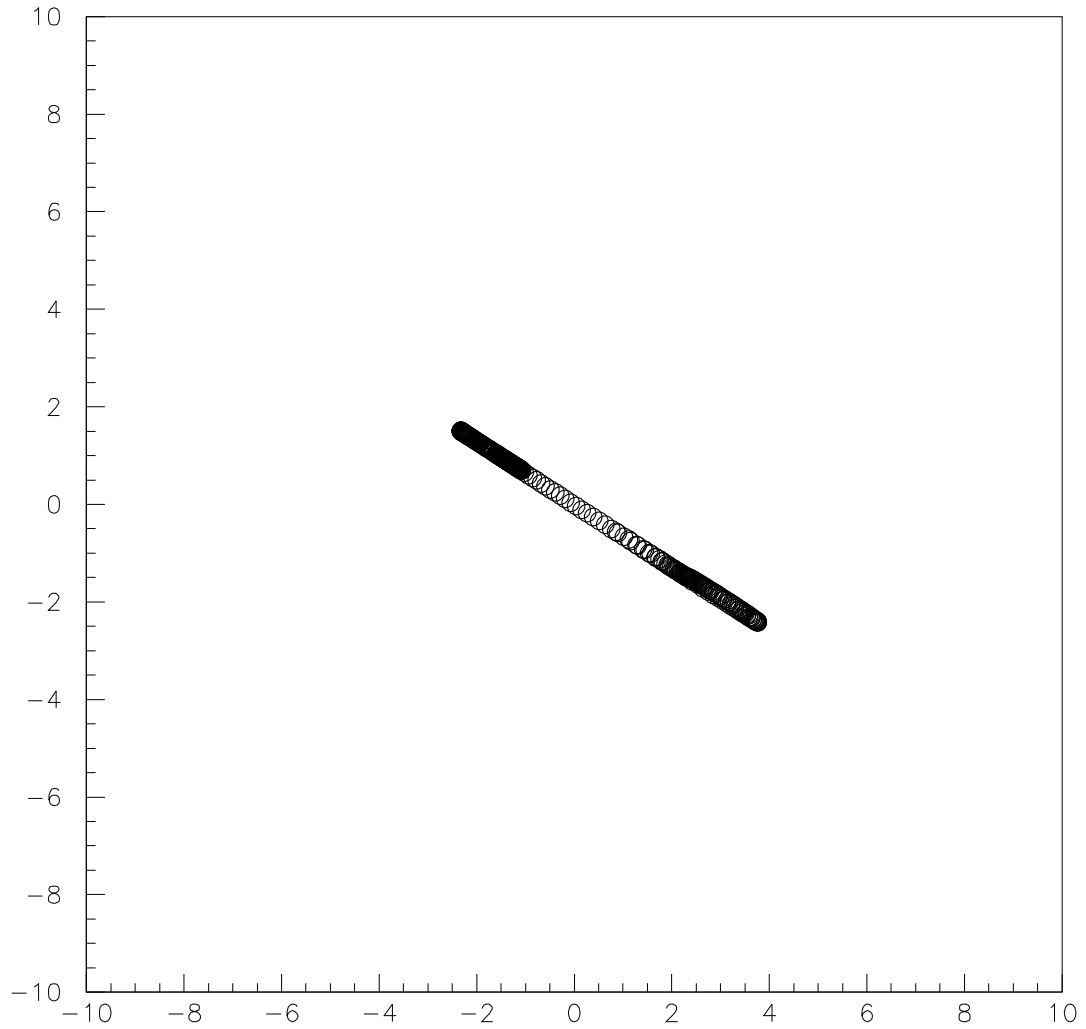


Figure 16: In the S-matrix $\eta \pi \pi$ to $\pi \pi$ there is a smooth background term which is used in equation 20(the fifth term). In the fit of equation 20 to the STAR high precision Au + Au ultra-peripheral coherent photoproduction data at $\sqrt{s_{NN}} = 200$ GeV(the highest RHIC energy) we obtain for the fifth term the above amplitude for the higher mass region 1.0 GeV to 1.9 GeV.

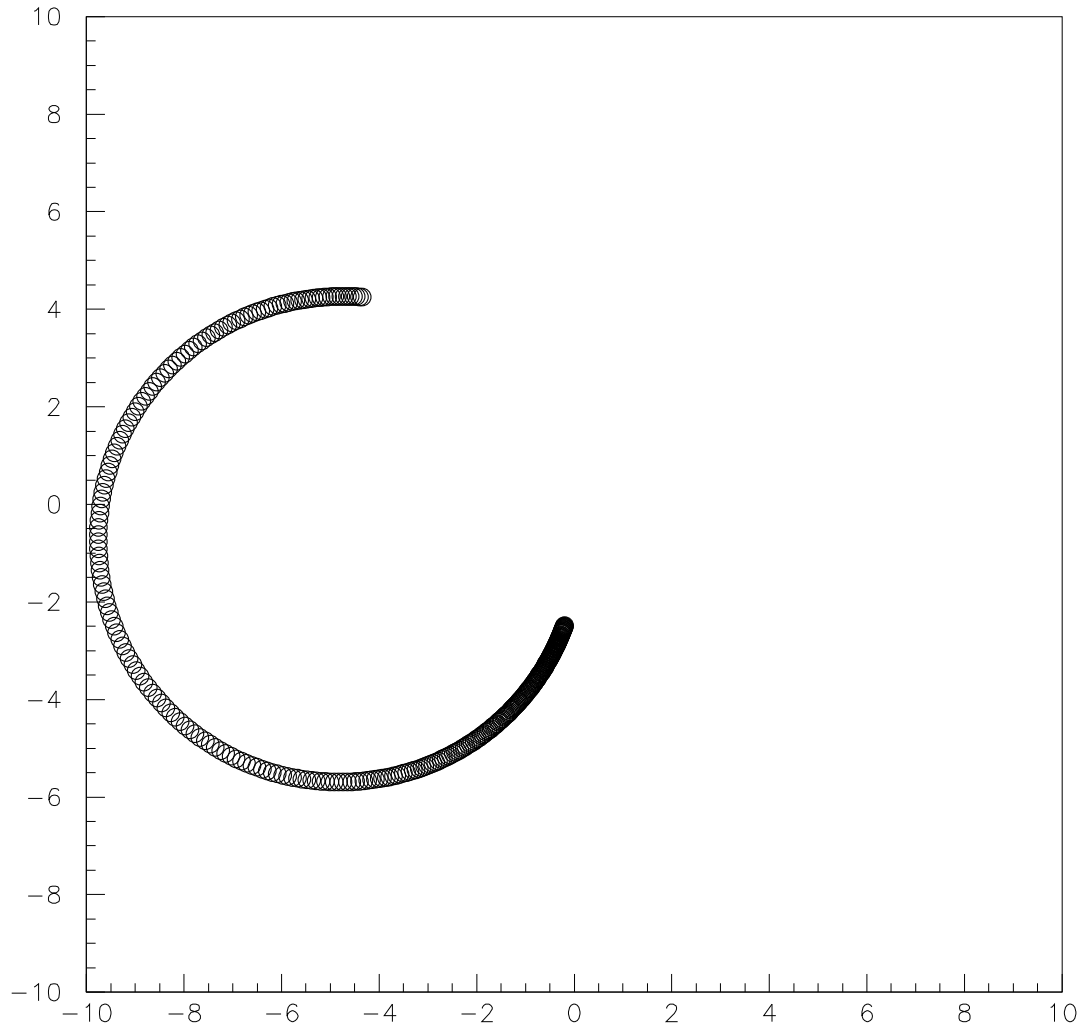


Figure 17: The Breit-Wigner pole($BW_1(\rho(1330))$) for the $\rho(1330)$ is used in equation 20(the sixth term). In the fit of equation 20 to the STAR high precision Au + Au ultra-peripheral coherent photoproduction data at $\sqrt{s_{NN}} = 200$ GeV(the highest RHIC energy) we obtain for the sixth term the above amplitude for the higher mass region 1.0 GeV to 1.9 GeV.

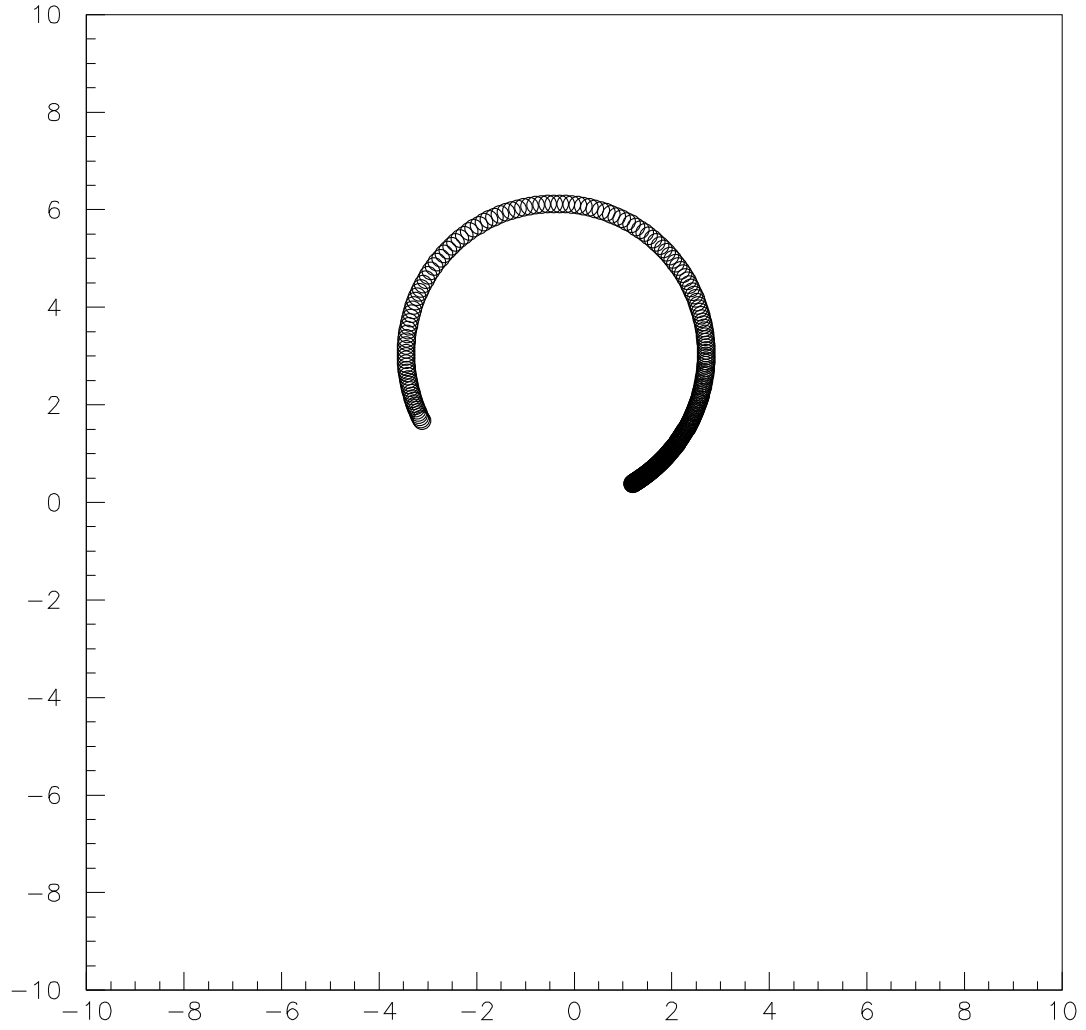


Figure 18: The Breit-Wigner pole($BW_3(\rho(1730))$) for the $\rho(1730)$ is used in equation 20(the seventh term). In the fit of equation 20 to the STAR high precision Au + Au ultra-peripheral coherent photoproduction data at $\sqrt{s_{NN}} = 200$ GeV(the highest RHIC energy) we obtain for the seventh term the above amplitude for the higher mass region 1.0 GeV to 1.9 GeV.

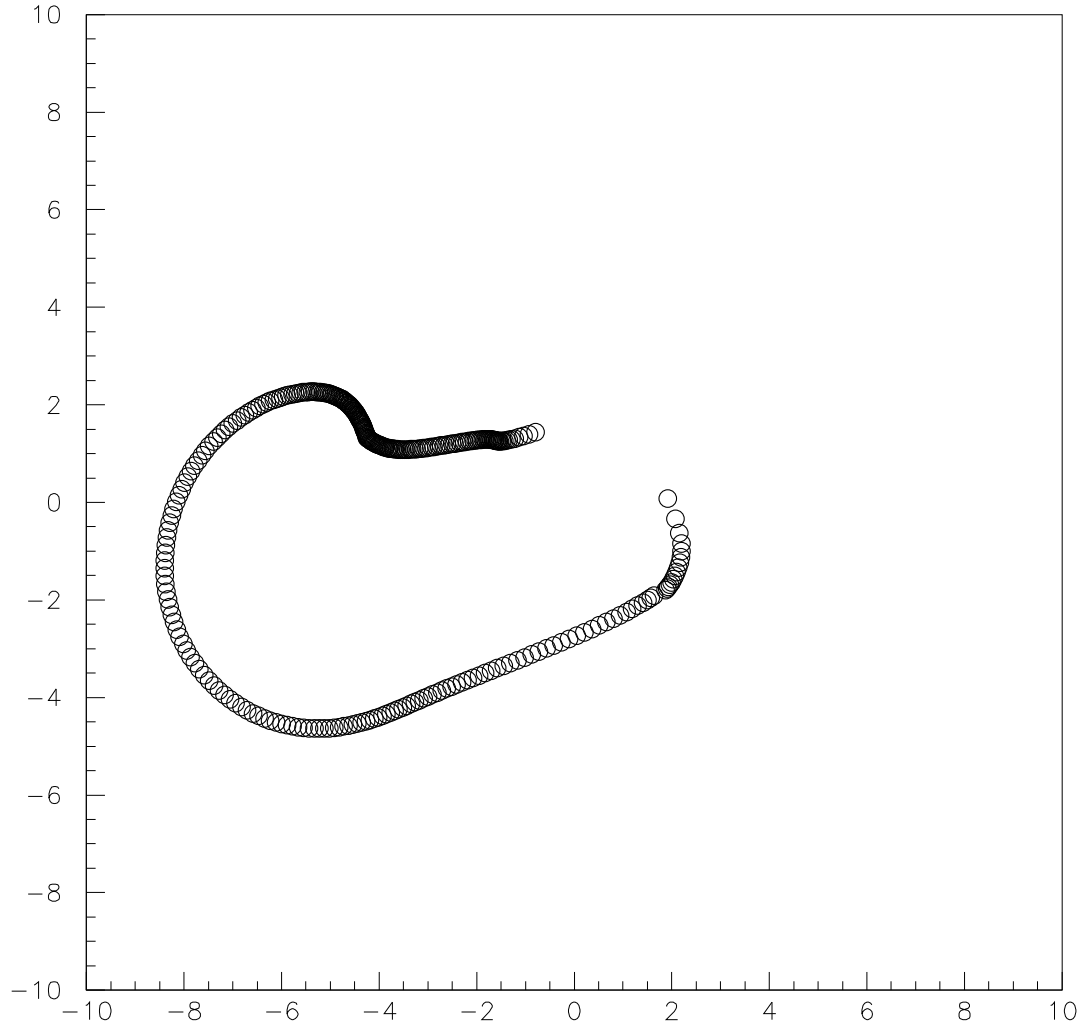


Figure 19: The unitary modified Breit-Wigner pole($B\tilde{W}_2\rho(1630)$) for the $\rho(1630)$ is used in equation 20(the eighth term). In the fit of equation 20 to the STAR high precision Au + Au ultra-peripheral coherent photoproduction data at $\sqrt{s_{NN}} = 200$ GeV(the highest RHIC energy) we obtain for the eighth term the above amplitude for the higher mass region 1.0 GeV to 1.9 GeV.

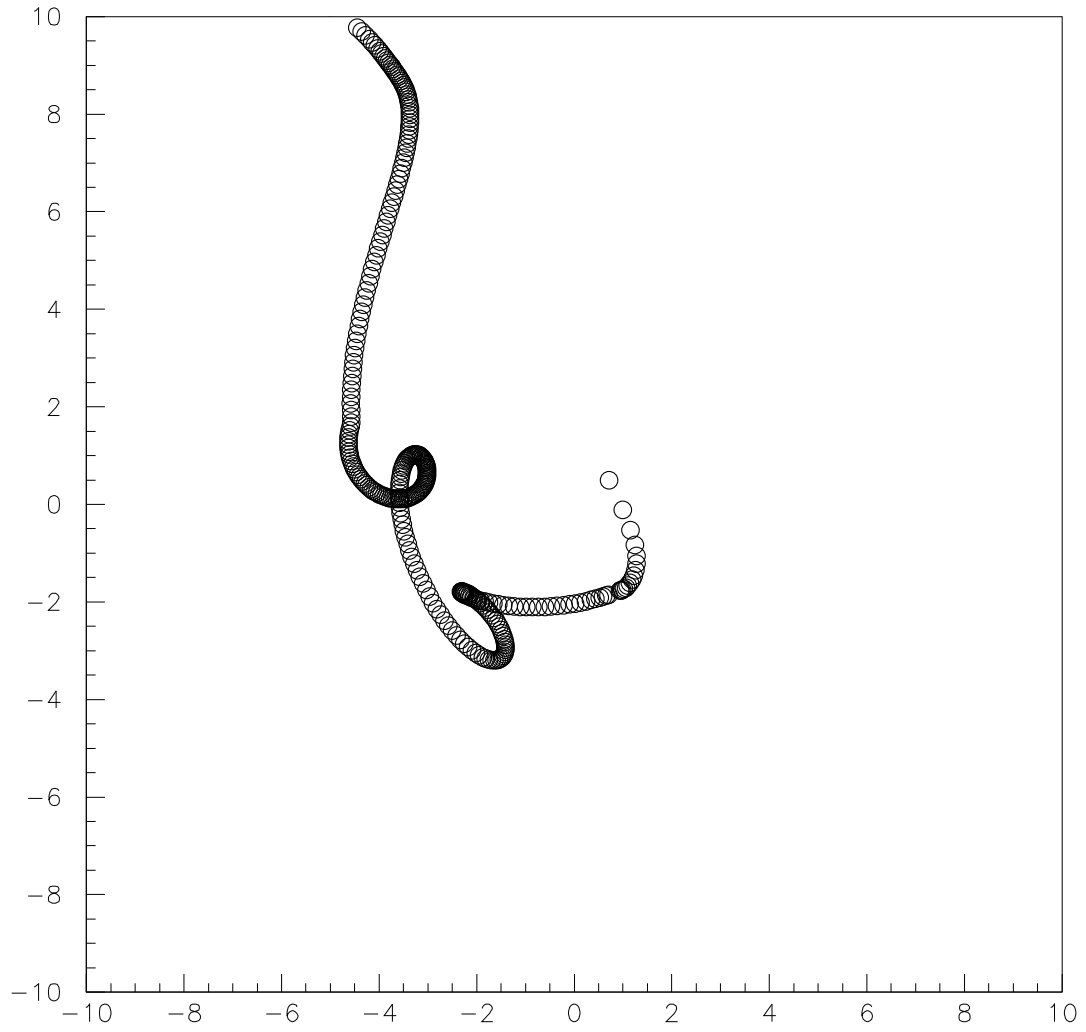


Figure 20: In the fit of equation 20 to the STAR high precision Au + Au ultra-peripheral coherent photoproduction data at $\sqrt{s_{NN}} = 200$ GeV (the highest RHIC energy) we obtain the above amplitude for the higher mass region 1.0 GeV to 1.9 GeV.

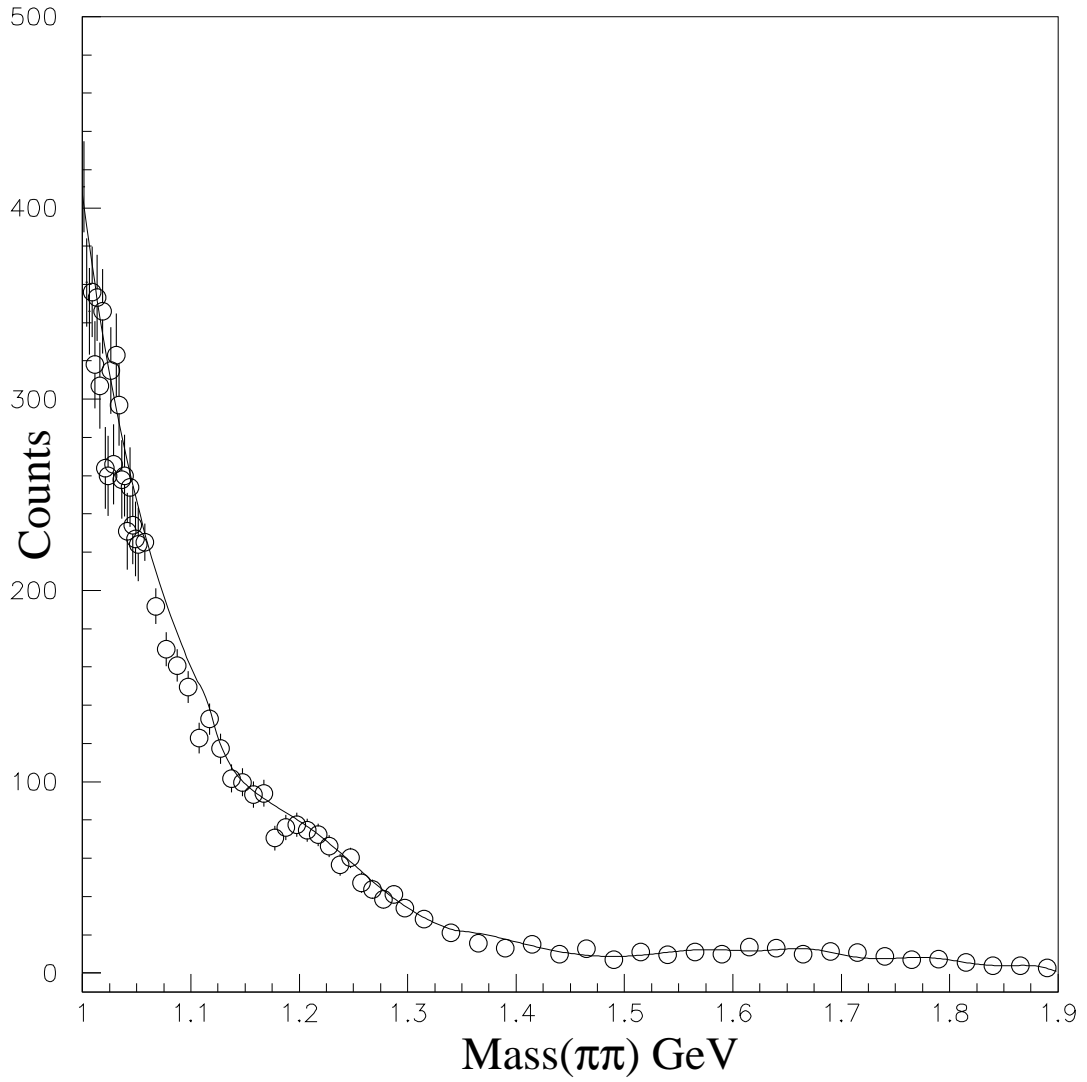


Figure 21: The fit to the STAR high precision Au + Au ultra-peripheral coherent photoproduction data at $\sqrt{s_{NN}} = 200$ GeV (the highest RHIC energy) for the higher mass region 1.0 GeV to 1.9 GeV with the amplitude coming from equation 20.

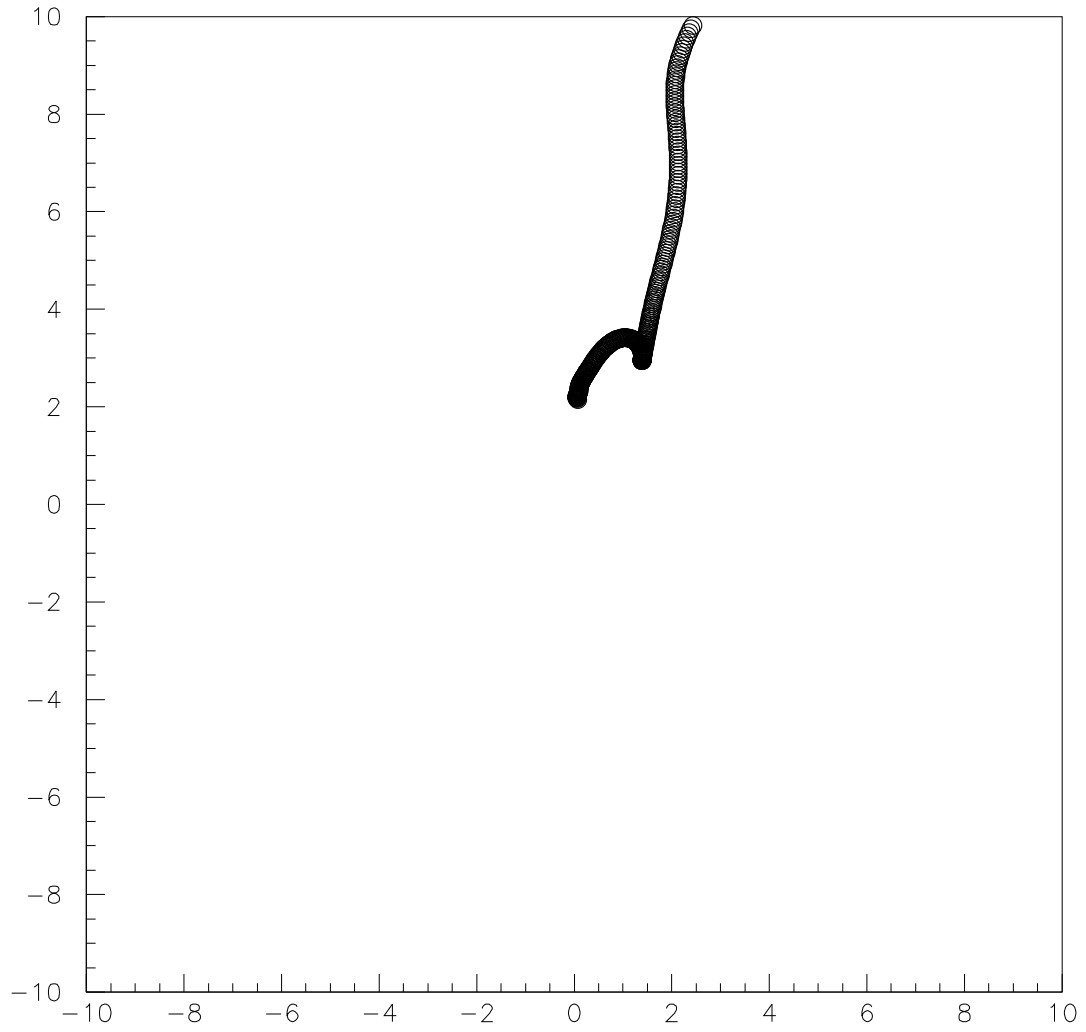


Figure 22: In the fit of the Söding Model to the STAR high precision Au + Au ultra-peripheral coherent photoproduction data at $\sqrt{s_{NN}} = 200$ GeV (the highest RHIC energy) we obtain the above amplitude for the higher mass region 1.0 GeV to 1.9 GeV.

The coherent photoproduction data are fitted using a generalized Söding Model[5] which is outlined in Figure 1. We see in the figure that there are two terms. One being a Söding background term of pion pairs coming directly out of the vacuum plus a second being the photon coupling directly to the 1^{--} scattering matrix. The universal lepton pair coupling through the photon gives use T_{31} as the direct coupling. We use the form for the Söding background term given by equation 12. The directly coupled term of the photon to the S-matrix is given by equation 13. The results of the global fit is shown in Figures 2 through 6. The overall χ^2 for the global fit which has 1669 degrees of freedom is 1926. The 1σ error on such a fit is a $\Delta\chi^2$ of 58. This implies that this global fit is 4.8σ away from a 1669 χ^2 fit.

We have achieve a global fit to the data sets which gives an analytic form for the S-matrix. Using this analytic form we search for poles in the 1^{--} S-matrix. In this search we find 5 poles. The first pole is the well know $\rho(760)$, while its isospin partner $\omega(780)$ is the second pole. In the high mass region one expects there should be two radial excitations of the $\rho(760)$. These excitation masses should be at around 1300 and 1800 MeV. One should also expect there should be a d-wave $q\bar{q}$ state at around 1600 MeV. We see the poles in the high mass are $\rho(1330)$, $\rho(1630)$ and $\rho(1730)$ which is consistent with this picture.

The Söding Model has a built-in term of interference between the direct production term and the background term. This interference term is equivalent to a re-scattering as shown in Figure 7. The re-scattering term is a loop of pions coming from the background and re-interacting with the S-matrix of $\pi\pi$ p-wave scattering. The loop or bubble has a real and a imaginary part. The imaginary part of the loop is equal to $B_{\pi\pi}$ (equation 12) times S-matrix $\pi\pi$ p-wave scattering. The real part of the loop is equal to $\alpha B_{\pi\pi}$ times S-matrix $\pi\pi$ scattering. The value of α is determined to be 2.0 in Ref.[6] from photo production data. Figure 7 and equation 14 gives the equation for the background plus re-scattering. To equation 14 we must add the direct production of the $\rho(760)$ pole and the $\omega(780)$ pole in the lower mass region. When this is done we break the constraint of the Söding Model that the $\omega(780)$ into $\pi\pi$ has to be the same as e^+e^- scattering to $\pi^+\pi^-$ [2]. With this added freedom the global fit χ^2 improve by 257 which a 4.8σ improvement(see Figure 8). This photo production amplitude into $\pi\pi$ is shown in Figure 9, while the Söding Model $\pi\pi$ amplitude is shown in Figure 10. Even though we have a quantitative difference these amplitudes are qualitatively the same.

In the higher mass region a new background becomes possible. In our model for the 1^{--} system we have a large coupling of the $\pi\pi$ channel to the $\eta\pi\pi$ channel. Thus if the photon directly produces the $\eta\pi\pi$ channel, then through a $\eta\pi\pi$ loop one can form the $\pi\pi$ channel by the cross term of the S-matrix of $\eta\pi\pi$ to $\pi\pi$ (see Figure 11). Again the loop or bubble has a real and a imaginary part. The imaginary part of the loop is equal to $B_{\eta\pi\pi}$ (equation 15) times T-matrix $\eta\pi\pi$ to $\pi\pi$ scattering. The real part of the loop is equal to $2.0 B_{\eta\pi\pi}$ times T-matrix $\eta\pi\pi$ to $\pi\pi$. Figure 11 and equation 16 gives the equation for the re-scattering.

We then perform a new global fit to the photoproduction data plus e^+e^- scattering to $\pi^+\pi^-$ [2] and $\pi^+\pi^-\pi^0$ [3] plus the p-wave partial wave analysis of $\pi^+\pi^-$ to $\pi^+\pi^-$. As part of this fit we use equation 14 and equation 16. Since the photoproduction data is the square of the amplitude there is an over all phase that is not determined. Let us choose equation

14 to determine this phase. The result of this fit gives a result for equation 14 which is displayed in Figure 12. The background rises quickly at threshold and then falls off with mass. The higher mass region is the focus of Figure 13. We see that the background term equation 14 for the pion loop is mainly a real function. Equation 16 which is the $\eta \pi \pi$ loop is also mainly real and of the same magnitude at these higher masses. This background also rises quickly at threshold and then falls off with mass tailing to zero(see Figure 14).

In the S-matrix in the higher mass region there are 3 poles plus the possibility of background terms when we consider T_{11} and T_{51} . Unitarity means that all of these terms must fit together and satisfy the unitary constraints. We are able to achieve such an unitary construction using an ad hoc step by step construction of first T_{11} and then T_{51} . The tail of the $\rho(760)$ meson extend into the high mass region tailing off to a small amplitude. We will denote this background as B_{11} . The shape of this background is shown in Figure 15. The poles for $\rho(1330)$ and $\rho(1730)$ have a very small coupling to the $\pi \pi$ channel. For these poles we use a Breit-Wigner form which has the same pole position as our k-matrix fit. Let us denote these forms as $BW_1(\rho(1330))$ and $BW_3(\rho(1730))$. We define the quasi factorizable Breit-Wigner form($B\tilde{W}_2$) through the equation 17. We then turn to the T_{51} amplitude and define a background term B_{51} in equation 18 with the constraint of equation 19. For the final fit to the high mass photoproduction data we use equation 20 which has eight terms((1and2) $\pi \pi$ loops; (3) $\eta \pi \pi$ loops; (4) T_{11} background; (5) T_{51} background; (6) $\rho(1330)$; (7) $\rho(1730)$; (8) $\rho(1630)$). The results of the eight terms are shown in figures 13 through 19 with the final sum being Figure 20 with the fit shown in Figure 21. The overall χ^2 for this global fit which has 1649 degrees of freedom is 1649. In the higher mass region we get an improvement of 20 in χ^2 . This is a better fit than before but not statistical significant. We can compare with the higher mass amplitude from the Söding Model fit which we show in Figure 22.

7 Acknowledgments

This research was supported by the U.S. Department of Energy under Contract No. DE-AC02-98CH10886.

8 Appendix

The T_{11} elastic scattering amplitude is a complex amplitude described by two real numbers one bounded between 0.0 and 1.0(η_1) and another is in units of angles(δ_1). The form of the amplitude is

$$T_{11} = \eta_1 \sin \delta_1 e^{i\delta_1} \quad (21)$$

We note that η_1 and δ_1 depends on the value of $M_{\pi\pi}$, and one could also use $\text{real}(T_{11})$ and $\text{imag}(T_{11})$.

In order to make a well controlled k-matrix calculation let us assume that above a $M_{\pi\pi}$ greater than 1.1 Gev/c there are two important channels 1 $\pi^+ \pi^-$ and 2 $\eta \pi^+ \pi^-$. Thus we

need a 2X2 k-matrix which we will assume is factorizable with two factors k_1 and k_2 such that

$$K_{11} = k_1 k_1, K_{12} = k_1 k_2, K_{21} = k_1 k_2, K_{22} = k_2 k_2. \quad (22)$$

The T_{11} elastic scattering amplitude is equal to

$$T_{11} = \frac{k_1^2}{1.0 - i(k_1^2 + k_2^2)}. \quad (23)$$

let us define

$$\alpha = (k_1^2 + k_2^2), \quad (24)$$

and rewriting the above equation we have

$$T_{11} = \frac{k_1^2}{1.0 - i\alpha}. \quad (25)$$

We multiply numerator and denominator by the complex conjugate of denominator of the above equation we obtain

$$T_{11} = \frac{k_1^2 + i\alpha k_1^2}{1.0 + \alpha^2}. \quad (26)$$

We see that

$$\frac{T_{11}}{k_1^2} = \frac{1.0 + i\alpha}{1.0 + \alpha^2}. \quad (27)$$

Thus the real part

$$\frac{Real(T_{11})}{k_1^2} = \frac{1.0}{1.0 + \alpha^2}, \quad (28)$$

and the imaginary part

$$\frac{Imag(T_{11})}{k_1^2} = \frac{\alpha}{1.0 + \alpha^2}. \quad (29)$$

Dividing equation 29 by 28, we obtain

$$\alpha = \frac{Imag(T_{11})}{Real(T_{11})}. \quad (30)$$

$$k_1^2 = (\text{Real}(T_{11}))(1.0 + \alpha^2). \quad (31)$$

$$k_2^2 = \alpha - k_1^2. \quad (32)$$

We can redefine the p-wave $\pi\pi$ phase shift into two real functions between 1.1 GeV to 1.9 GeV. If define a new variable x such that

$$x = 2.5M_{\pi\pi} - 3.75. \quad (33)$$

Over the $M_{\pi\pi}$ range 1.1 GeV to 1.9 GeV, x varies from -1.0 to 1.0. Therefore we can expand the two real functions k_1 and k_2 in terms of Legendre polynomials. We project out these polynomials up to 9th order and use these values to start the global fits described in the text.

References

- [1] L. Adamczyk *et al.*, Phys. Rev. C 96 (2017) 054904.
- [2] M.N. Achasov *et al.*, arXiv:0605013[hep-ex].
- [3] M.N. Achasov *et al.*, arXiv:0305049[hep-ex].
- [4] B. Hyams, C. Jones, P. Weilhammer, Nucl. Phys. B 96 (1973) 134-162.
- [5] P. Söding, Phys. Lett. 19 (1966) 702.
- [6] R.S. Longacre, arXiv:1306.2908[Nucl-th].